RSC Advances

PAPER

Check for updates

Cite this: *RSC Adv.*, 2021, **11**, 3202

Hydrothermal synthesis of a novel nanolayered tin phosphate for removing Cr(III)†

Wei-Qi Li, Duan Liu, Ji-Yan Qu and Jian-Hong Luo *

Received 15th October 2020
Accepted 23rd December 2020

DOI: 10.1039/d0ra08775k

rsc.li/rsc-advances

In this work, an outstanding nanolayered tin phosphate with 15.0 Å interlayer spacing, Sn $(HPO_4)_2 \cdot 3H_2O$ (SnP–H^+), has been synthesized by conventional hydrothermal method and first used in the adsorptive removal of Cr(III) from aqueous solution. A number of factors such as contact time, initial concentration of Cr(III), temperature, pH, and ionic strength on adsorption were investigated by batch tests. Moreover, the isothermal adsorption characteristics and kinetic model of Cr(III) onto SnP–H^+ were studied. The results showed that the adsorption of Cr(III) by SnP–H^+ was in accordance with the Langmuir adsorption isotherm model and the pseudo-second-order kinetic model. The adsorption capacity of Cr(III) onto SnP–H^+ at temperature 40.0 °C and pH 3.0 could reach 81.1 mg g^{-1}. And the distribution coefficient K_d was 23.0 g L^{-1}. Overall, experiments certified that SnP–H^+ was an excellent adsorbent that can effectively remove Cr(III) from aqueous solution.

1. Introduction

Many industrial production activities such as leather tanning, electroplating, metal refining, metallurgy, and so on will produce chromium-containing wastewater resulting in water environment pollution.[1–3] Chromium is a transition metal that has several oxidation states, but chromium trivalent and chromium hexavalent are the most stable.[2] Cr(III) is an essential trace element for the growth of many organisms.[4] However, Cr(VI) is a highly toxic substance that can cause many diseases through the skin, respiratory and digestive tracts.[2,5–7] Although trivalent chromium is beneficial to the life activities of organisms, excess chromium is toxic and harmful.[5,8] The fact that chromium changes rapidly from trivalent to hexavalent have been proved by a group of researchers.[9] Therefore, chromium must be removed as much as possible from industrial wastewater with the complex matrix before discharging.[10–14] The methods of removing chromium from aqueous solutions include precipitation, ion exchange, reduction, electrochemical precipitation, solvent extraction, membrane separation, adsorption, *etc.*[15] Among them, adsorption is an important method to treat wastewater containing heavy metals with high efficiency, low cost and simple operation.[6] However, due to being short of appropriate adsorbents with excellent adsorption properties, such as traditional adsorbent activated carbon, this method is still limited in application.[16] Organic ion exchangers such as ion exchange resins have limited chemical, thermal and radiation stability, which makes them unsuitable for the harsh wastewater environment in practice. In recent years, many researches on inorganic layered ion exchangers have been performed, including layered double hydroxides,[17] layered metal oxides,[18] and layered metal sulfides.[19] These materials show potential applications because of their simple preparation, excellent chemical stability, rich composition and structure, and strong ion exchange ability.[20–28]

Considering the special structure of SnP–H^+ and the less application of layered phosphate in trivalent chromium removal technology, this paper mainly studied the effect of conventional hydrothermal synthesis SnP–H^+ in the removal of Cr(III) in aqueous solution. The effects of adsorption time, initial concentration of Cr(III), temperature, pH, and ionic strength on the adsorption of Cr(III) onto SnP–H^+ will be researched. Thus, the effective conditions for the adsorption of Cr(III) with a low concentration on SnP–H^+ were obtained.

2. Experimental

2.1 Materials

The reagents used in this study were all of the analytical grade. NaH_2PO_4 (99.0%) and concentrated HCl (36.0–38.0%) were supplied by Chengdu Kelong Chemical Co., Ltd., China. $SnCl_4 \cdot 5H_2O$ (99.99%) and $Cr(NO_3)_3 \cdot 9H_2O$ (99.0%) were purchased from Aladdin Chemistry Co., Ltd., China.

2.2 Characterization

The SnP–H^+ was investigated by X-ray diffractometer (XRD, Panalytical, EMPYREAN), high resolution transmission electron microscopy (HRTEM, Tecnal G^2 F20), and thermal analysis (METTLER TOLEDO, TGA-DSC2/1600), respectively.

Dep. of Chemical Engineering, Sichuan University, Chengdu, Sichuan, 610065, China. E-mail: luojianhong@scu.edu.cn

† Electronic supplementary information (ESI) available. See DOI: 10.1039/d0ra08775k

This article is licensed under a Creative Commons Attribution-NonCommercial 3.0 Unported Licence.

(cc) BY-NC

© 2021 The Author(s). Published by the Royal Society of Chemistry

XRD (Cu-target) pattern was collected with Kα1 radiation of wavelength $\lambda = 1.540598$ Å and Kα2 radiation of wavelength $\lambda = 1.544426$ Å. Scan speed of 1 s per step and step size of 0.03°. HRTEM image was obtained by Tecnal G2 F20 operated at 200 kV. TGA and DSC were carried out with a heating rate of 10 °C min^{-1}.

2.3 Preparation of SnP–H^+

The synthesis method is similar to the microwave hydrothermal synthesis of SnP–H^+.[29] 5 mL of 1 M $SnCl_4$ in 1 M HCl and 20 mL of 3 M NaH_2PO_4 were mixed fully in 100 mL Teflon-lined stainless steel autoclave. The pH was adjusted to 0.4 with concentrated hydrochloric acid and then reacted at 195.0 °C hydrothermal for 48 hours. The product after cooling was washed 4 times with 1 M HCl and deionized water, respectively. The final samples were obtained after centrifugation and dried at 60 °C for 5 hours.

2.4 Adsorption experiments

Certain amounts of $Cr(NO_3)_3 \cdot 9H_2O$ were dissolved in deionized water to prepare a series of solutions of different concentrations (10.0, 20.0, 30.0, 40.0, 50.0 mg L^{-1}). Afterward, batch adsorption experiments were performed by contacting 10 mg of SnP–H^+ with aqueous solutions of different initial concentrations of Cr(III) (40 mL) in sealed 150 mL triangular flasks, which determined the effect of contact time on adsorption capacity. Subsequent experiments confirmed the adsorption capacity of SnP–H^+ in a low concentration of Cr(III) at different temperatures (25.0, 30.0, 35.0, 40.0, 45.0 °C) and pH (1.0, 1.5, 2.0, 2.5, 3.0, 3.7). All the above adsorption operations were conducted in a thermostatic oscillator with a speed of 140 rpm. The content of Cr(III) in the supernatant after centrifugation was measured by atomic absorption spectrometry (AAS). The measurements of the chromium concentration in the studied were performed using flame atomic absorption spectrophotometer (SHIMADZU, AA-6880). A hollow cathode lamp (Shimadzu (Shanghai) Global Laboratory Consumables Co., Ltd) was used for the measurement of chromium concentration with a lamp current of 10 mA. The wavelength of 357.9 nm and slit width of 0.7 nm were selected for the measurement. Moreover, the values of acetylene and air flow, the basic spectrometer parameters, were 2.8 and 15 L min^{-1} respectively. The limit of Cr detection was at the level of 0.13 mg L^{-1}.

The adsorption capacity (q_e, mg g^{-1}) of Cr(III) on SnP–H^+ at equilibrium and the amount adsorbed per unit mass of the SnP–H^+ at time t (q_t, mg g^{-1}), as well as the distribution coefficient (K_d, L g^{-1}) were respectively calculated by the following eqn (1)–(3):

$$q_t = \frac{(C_0 - C_t) \times V}{m} \quad (1)$$

$$q_e = \frac{(C_0 - C_e) \times V}{m} \quad (2)$$

$$K_d = \frac{[(C_0 - C_e) \div C_e] \times V}{m} \quad (3)$$

where C_0 (mg L^{-1}) is the initial concentration of Cr(III); C_t (mg L^{-1}) and C_e (mg L^{-1}) are the concentration of Cr(III) at time t and adsorption equilibrium; V (L) is the volume of the solution; m (g) is the amount of SnP–H^+ used in the experiment. K_d (L g^{-1}) is the ratio of the amount of Cr(III) adsorbed by one gram of adsorbent to the amount of Cr(III) remaining in the solution. When the K_d of a certain adsorbent is greater than or equal to 10.0 L g^{-1}, it is regarded as a superior adsorbent.[16]

The removal efficiency (R) is expressed as:

$$R = \frac{C_0 - C_e}{C_0} \times 100\% \quad (4)$$

2.5 Desorption experiments

The samples used in desorption experiments was prepared by using a solution of 20 mg L^{-1} of Cr(III) at pH 3.0 in contact with 10 mg of sorbent, at 25 °C for 40 min. The samples were then filtered and placed in an oven at 60 °C for 2 h. Then 8 mg dried sample was contacted with 20 mL HCl (1 or 3 M), HNO_3 (1 or 3 M) and H_2SO_4 (1 or 3 M) solutions respectively in a closed 150 mL conical flask. The conical flask shaked at 25 °C for 24 h. After the desorption experiments, the samples were filtered and the content of Cr(III) in the liquid was analyzed. The desorption efficiency, R_{des} (%) was calculated as follows:

$$R_{des} = \frac{C_{des} \times V}{q_e m_{des}} \quad (5)$$

where C_{des} (mg L^{-1}) is the concentration of Cr(III) and m_{des} (g) is the amount of sample in the desorption experiments.

3. Results and discussion

3.1 Characterization

The XRD pattern is shown in Fig. 1. The main peak of the synthesized phosphate is at 15.1 Å. This is consistent with the report in the previous article,[29] which proves that we synthesized a nanolayered tin phosphate with 15.0 Å interlayer spacing. The HRTEM in Fig. 2(a)–(c) displays that lattice fringes with a plane spacing of 0.375, 0.751 and 0.292 nm respectively. An identical conclusion is obtained in the XRD pattern. As we can see from Fig. 3, the weight loss of SnP–H^+ reaches 11.4% at 225.6 °C, that is, about 2.2 moles of water molecules are released.[30] Besides, we observe that the peak at 3.4 Å in the XRD pattern belongs to anhydrous tin phosphate. Thus, we think the synthesized sample should be a mixture of anhydrous tin phosphate and SnP–H^+.

3.2 Effect of contact time

Fig. 4 shows that the influence of contact time on adsorption of Cr(III) different concentrations on SnP–H^+. The adsorption on SnP–H^+ reached adsorption equilibrium at an initial concentration of 10.0 mg L^{-1} after 10 minutes. The highest removal efficiency of Cr(III) was 96.9%. As for the initial concentrations of Cr(III) from 20.0 to 50.0 mg L^{-1}, the removal efficiency was stable after 40 minutes. Moreover, it was observed that all the

© 2021 The Author(s). Published by the Royal Society of Chemistry

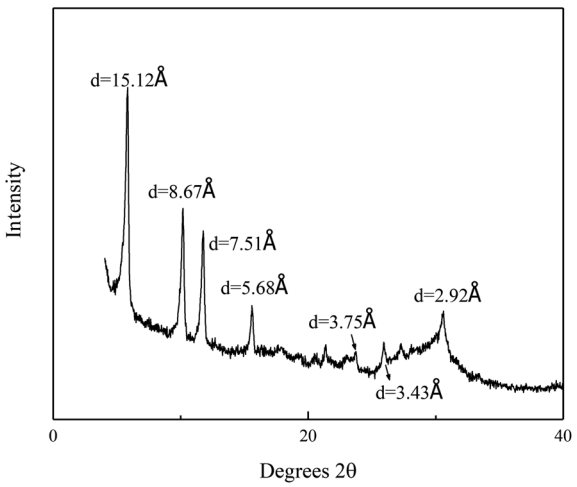

Fig. 1 XRD pattern of SnP–H^+.

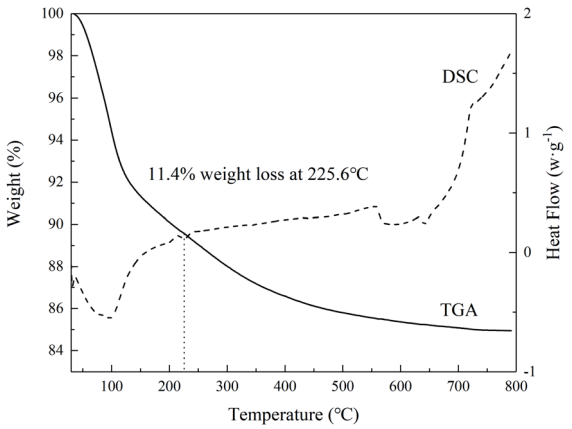

Fig. 3 DSC-TGA curves of SnP–H^+.

curves rose rapidly in the first 10 minutes, which indicates that the adsorption rate increased rapidly at this stage. This is due to a higher interlayer spacing of SnP–H^+, which makes it easier for hydrated protons with larger diameters to exchange with Cr^{3+}.[29] The adsorption capacity of the adsorbent for Cr(III) with various initial concentrations of Cr(III) (20.0–50.0 mg L^{-1}) increased slowly after 10 minutes until the adsorption was steady. With the increase over time, the number of switching bits available in SnP–H^+ decreases, resulting in a slow increase in removal efficiency.

3.3 Effect of initial concentration of Cr(III)

The effect of initial concentration of Cr(III) (10.0–50.0 mg L^{-1}) on adsorption is presented in Fig. 5 and S1.† The removal efficiency was 96.9% with the initial concentration of Cr(III) at 10.0 mg L^{-1}, and then decreasing to 34.5% when the concentration was 50.0 mg L^{-1}. In the case of the same quality of adsorbent, the adsorption capacity increases with the initial concentration of Cr(III). Higher concentrations of Cr(III) provide an important driving force for overcoming mass resistance between the water phase and the solid phase, causing an enhancement of the adsorption process.[31]

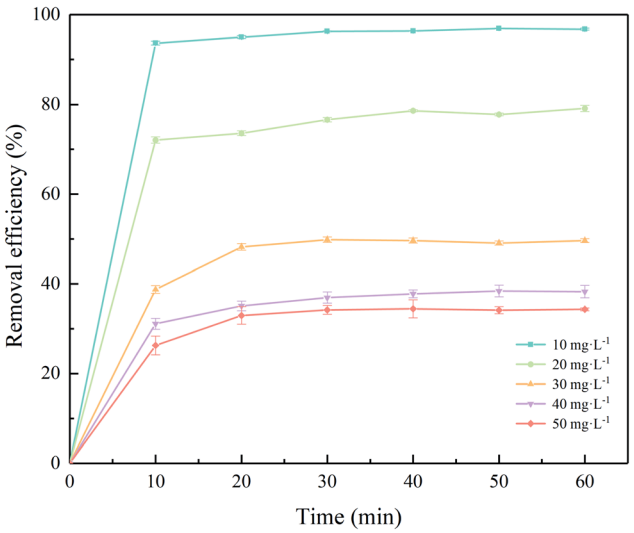

Fig. 4 Effect of contact time on the adsorption of different initial Cr(III) concentration onto SnP–H^+ at 25.0 °C.

3.4 Effect of temperature

It is known that an increasing temperature will increase the diffusion rate of adsorbate molecules on the outer boundary

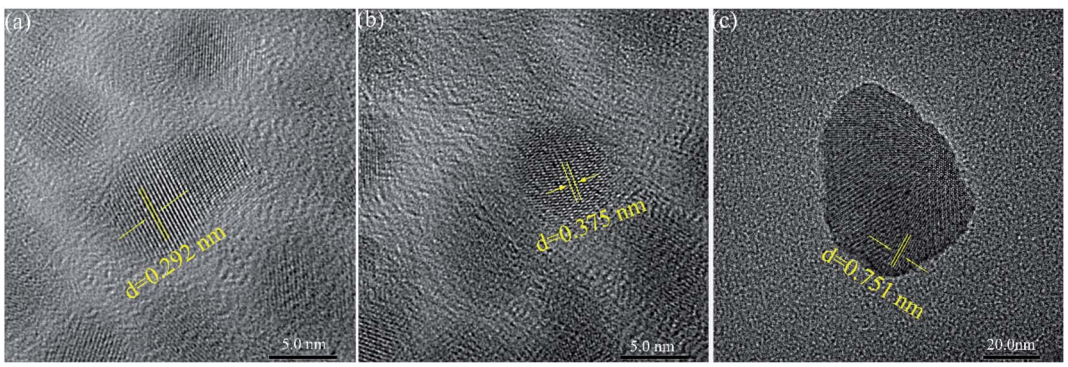

Fig. 2 TEM image (a)–(c) of SnP–H^+ at high magnification.

© 2021 The Author(s). Published by the Royal Society of Chemistry

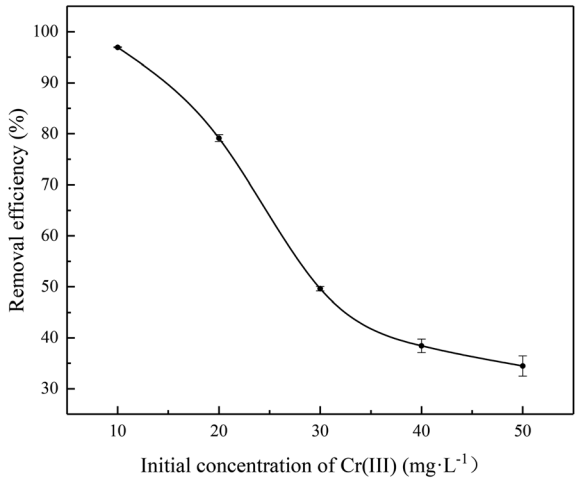

Fig. 5 Effect of initial concentration on the adsorption of Cr(III) onto SnP–H^+ at 25.0 °C.

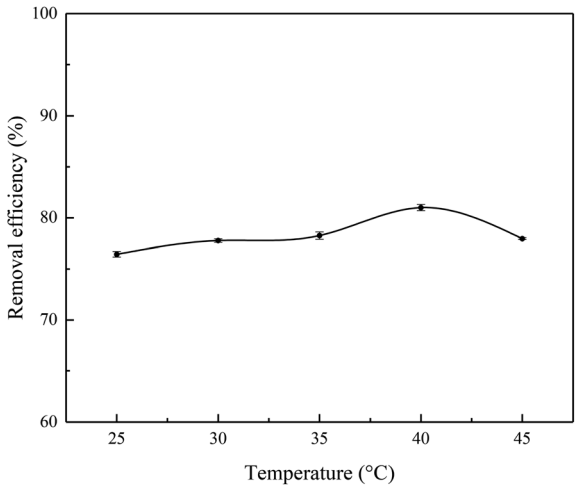

Fig. 6 Effect of temperature on the adsorption of Cr(III) onto the SnP–H^+ (adsorption conditions: initial concentration = 20.0 mg L^{-1}, contact time = 40 min, pH = 3.7).

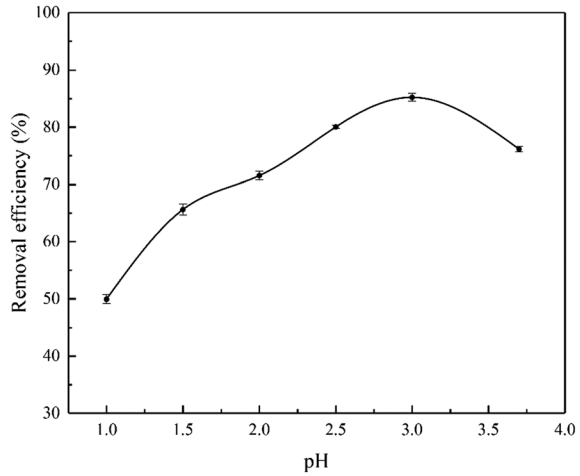

Fig. 7 Effect of pH on the adsorption of Cr(III) onto SnP–H^+ (adsorption conditions: temperature = 40.0 °C, initial concentration = 20.0 mg L^{-1}, contact time = 40 min).

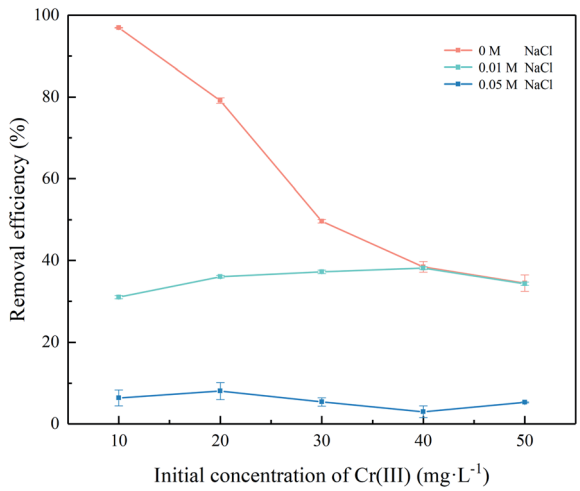

Fig. 8 Effect of pH on the adsorption of Cr(III) onto SnP–H^+ (adsorption conditions: temperature = 40.0 °C, initial concentration = 20.0 mg L^{-1}, SnP–H^+ dosage was 0.25 g L^{-1}, contact time = 40 min, pH = 3.0, and NaCl concentration ranged from 0.01 to 0.05 M).

layer. Changing the temperature will result in a change in the equilibrium capacity of a specific adsorbent.[32] Fig. 6 shows that temperature obviously affected the adsorption of Cr(III) on SnP–H^+. The removal efficiency of SnP–H^+ increased slowly from 25.0 to 40.0 °C, reaching the maximum removal efficiency of 81.0% at 40.0 °C. Then it decreased as the temperature increased (40.0–45.0 °C). The increase of removal efficiency indicates that the adsorption process has endothermic properties.[33] The decrease in removal efficiency with the increases of temperature, which may because of the weakening of the adsorption force between the adsorbent and Cr(III).[34]

3.5 Effect of pH

The pH of solution is regarded as an important factor affecting the adsorption of heavy metals because it can affect the speciation of metal ions and the surface properties of adsorbents.[35]

Taking into account the synthesis conditions of SnP–H^+ and the pH of the solution with the initial concentration of Cr(III) at 20.0 mg L^{-1} is 3.7. And owing to most of acidic chromium-containing wastewater, the pH range we measured in the experiments were from 1.0 to 3.7. Fig. 7 displays that pH had a signification influence on the adsorption capacity of the SnP–H^+. As we can see, the adsorption ability of the SnP–H^+ increased gradually in the pH range of 1.0–3.0, but then decreased when the pH continued to rise. At a pH of 3.0, the maximum removal efficiency of the adsorbent was 85.2%. And the distribution coefficient K_d was 23.0 g L^{-1} much greater than 10.0 g L^{-1} at this moment. Under the condition of lower pH, excessive protons compete with Cr(III) for adsorption sites that may result in a reduced adsorption ratio. As pH increases, the number of protons in the solution decreases, making metal ions

© 2021 The Author(s). Published by the Royal Society of Chemistry

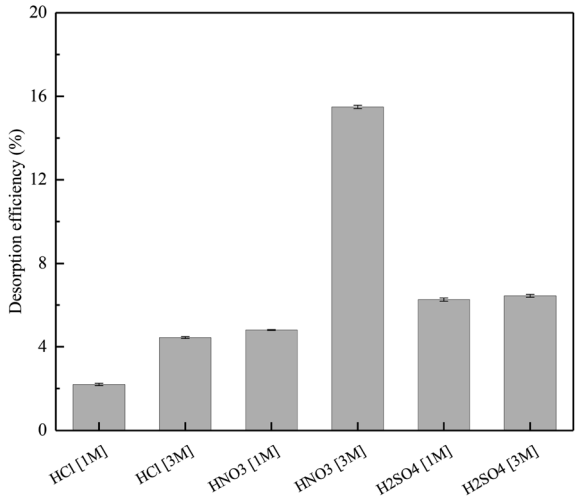

Fig. 9 Cr(III) desorption efficiency after 24 h washing of the SnP–H^+ with several eluents.

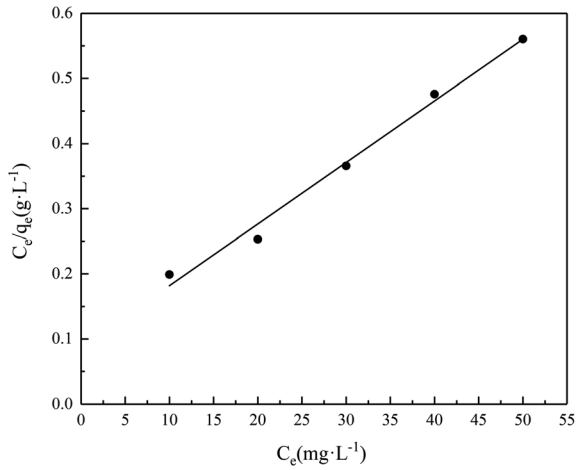

Fig. 10 Isotherm plot for Cr(III) adsorption by SnP–H^+ at the fitting of Langmuir isotherm model (adsorption conditions: temperature = 25.0 °C, contact time = 40 min).

Table 1 Langmuir and Freundlich constants for the adsorption of Cr(III) on SnP–H^+ at 25.0 °C[a]

Model	Constants	Cr(III)
Langmuir model	$q_{m,cal}$ (mg g^{-1})	105.3
	K_L (L mg^{-1})	0.1088
	R^2	0.9892
Freundlich model	n	2.97
	K_f ($mg^{-(n+1)/n}$ $L^{1/n}$ g^{-1})	25.12
	R^2	0.8568

[a] Where $q_{m,cal}$ (mg g^{-1}) is the theoretical maximum adsorption capacity of SnP–H^+.

more likely to be adsorbed.[36] When the pH is higher than 3, the amount of $CrOH^{2+}$, $Cr(OH)^{2+}$, $Cr_2(OH)_2^{4+}$, and $Cr_3(OH)_4^{5+}$ formed by hydrolysis of Cr^{3+} will increase.[37] The diameter of Cr-hydroxyl ion is larger than that of Cr^{3+}. Thus, the exchange between Cr^{3+} and hydrated proton may become difficult, leading to a weakened removal efficiency of SnP–H^+.

Table 2 Comparison of the adsorption capacity of SnP–H^+ for Cr(III) with different forms of adsorbent

Adsorbent	Adsorption capacity (mg g^{-1})	References
Ferrihydrite	53.14	45
Cus·PPP-SH	52.30	46
Na-Bent	6.44	47
Polyacrylamide–montmorillonite	59.74	48
Nitrolite	2.39	49
Ettringite	58.80	50
8-PTO	92.00	51
Boehmite nanoplates	19.85	52
SnP–H^+	105.30	This study

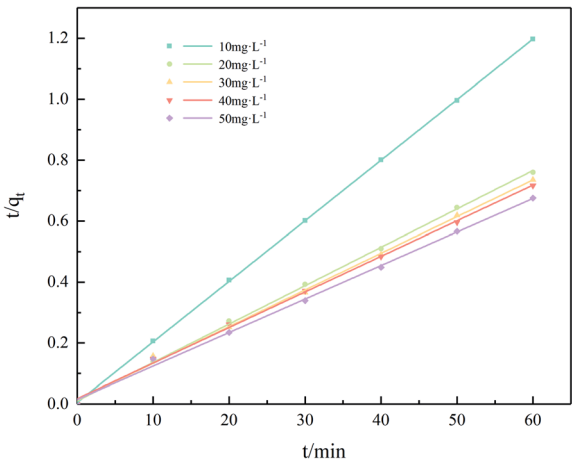

Fig. 11 The fitting plots of the pseudo-second-order kinetic model for Cr(III) adsorption on SnP–H^+.

3.6 Effect of ionic strength

Chrome-containing industrial wastewater often contains plenty of salt, and sodium chloride in tannery wastewater has been identified as one of the main pollutants.[38] Fig. 8 shows the effect of sodium chloride concentration on adsorption of Cr(III) onto the SnP–H^+. As the concentration of sodium chloride increased from 0 to 0.05 M, the equilibrium adsorption capacity decreased significantly. The presence of Na^+ may cause steric hindrance to Cr(III) with a large radius, leading to a decrease in the adsorption capacity of Cr(III) on the SnP–H^+.[39] The stronger ionic strength results in the preemption of more active sites by Na^+, thus reducing the equilibrium adsorption capacity of Cr(III) on the SnP–H^+.

3.7 Desorption experiments

The desorption of Cr(III) from SnP–H^+ using different kinds and concentrations of acid solutions was studied. The results of desorption efficiency could obtained by Fig. 9. When the

© 2021 The Author(s). Published by the Royal Society of Chemistry

Table 3 Kinetics parameters adsorption of Cr(III) on SnP–H^+ at 25 °C

Experiment		Pseudo-first-order kinetics			Pseudo-second-order kinetics		
C_0 (mg L^{-1})	q_e (mg g^{-1})	K_1 (min^{-1})	$q_{e,cal}$ (mg g^{-1})	R^2	K_2 (g mg^{-1} min^{-1})	$q_{e,cal}$ (mg g^{-1})	R^2
10.0	50.2	0.062	3.0	0.9619	0.079	50.3	0.9999
20.0	79.0	0.056	12.7	0.7159	0.015	79.4	0.9993
30.0	82.0	0.067	17.3	0.7432	0.011	83.3	0.9980
40.0	84.0	0.082	37.0	0.9998	0.008	85.5	0.9984
50.0	89.2	0.069	19.1	0.7815	0.008	90.9	0.9977

concentration of acid solution was 1 M, the desorption efficiency of sulfuric acid (6.3%) was the highest, followed by nitric acid (4.8%) and hydrochloric acid (2.2%). The concentration of acid solution increased from 1 to 3 M, and the desorption efficiency was improved to different degrees which nitric acid increased the most. In addition, the desorption efficiency of Cr(III) ranked as: HNO_3 (15.5%) > H_2SO_4 (6.5%) > HCl (4.8%). The above results indicate that the desorption of Cr(III) from SnP–H^+ is not complete which means better retention of Cr(III) by the SnP–H^+ phase.

3.8 Adsorption isotherm

The adsorption isotherm is a curve plotted by q_e and different initial concentrations of adsorbate (C_e).[16] Langmuir[40] and Freundlich[41] isotherm models are respectively expressed by the following eqn (6) and (7):

$$\frac{C_e}{q_e} = \frac{C_e}{q_m} + \frac{1}{K_L q_e} \quad (6)$$

$$\lg q_e = \frac{1}{n}\lg C_e + \lg K_f \quad (7)$$

where q_m (mg g^{-1}) is the maximum adsorption capacity of SnP–H^+, K_L (L mg^{-1})is the Langmuir constant, K_f ($mg^{-(n+1)/n}$ $L^{1/n}$ g^{-1}) is the Freundlich constant, and n is a constant related to sorption intensity.

The adsorption of Cr(III) on SnP–H^+ was studied by Langmuir and Freundlich isotherms and the results are shown in Fig. 10 and S2,† respectively. The isotherm parameters calculated by Langmuir and Freundlich model were listed in Table 1. Evidently, the correlation coefficient of the Langmuir model (R^2 = 0.9892) was higher than that of the Freundlich model (R^2 = 0.8568). Thus the Langmuir model was fitted better. This result confirms that the adsorption on SnP–H^+ is monolayer adsorption.[37,42]

According to the Langmuir model, the maximum adsorption capacity of Cr(III) on SnP–H^+ was 105.3 mg g^{-1}. Compared with the maximum adsorption capacity of Cr(III) on other adsorbents in literatures, SnP–H^+ has excellent adsorption efficiency (see Table 2).

3.9 Adsorption kinetics

The adsorption kinetics of Cr(III) with different concentrations on SnP–H^+ were described by pseudo-first order[43] (eqn (8)) and pseudo-second order[44] model (eqn (9)):

$$\ln(q_e - q_t) = \frac{1}{n}\ln q_e + K_1 \quad (8)$$

$$\frac{t}{q_t} = \frac{t}{q_e} + \frac{1}{K_2 q_e^2} \quad (9)$$

where K_1 (min^{-1}) and K_2 (g mg^{-1} min^{-1}) are pseudo-first order and pseudo-second order rate constants.

Fig. S3† and 11 show the pseudo-first order and pseudo-second order curves, respectively. Kinetics parameters adsorption of Cr(III) on SnP–H^+ are listed in Table 3. The above date illustrates that the correlation coefficient of pseudo-second order ($R^2 \geq 0.9977$) is higher than that of the pseudo-first-order model ($R^2 \geq 0.7159$). Hence the adsorption of Cr(III) on SnP–H^+ is more consistent with the quasi-second-order model. Therefore, the adsorption is more in line with the pseudo-second-order model. In addition, the theoretical maximum adsorption capacity of SnP–H^+ calculated by the pseudo-second order kinetic model basically conformed to the experimental value, indicating that the adsorption of Cr(III) on SnP–H^+ is chemical adsorption.[44]

4. Conclusions

In this study, the adsorption capacity of low concentration Cr(III) on the SnP–H^+ under different conditions was investigated. It is illustrated that the maximum adsorption capacity of Cr(III) with initial concentration at 20.0 mg L^{-1} was 81.1 mg g^{-1} at temperature 40.0 °C and pH 3.0 through batch experiments. The adsorption of Cr(III) on SnP–H^+ accords with Langmuir isotherm model and pseudo-second order kinetic model. In general, SnP–H^+ has the potential for practical application of Cr(III) adsorption in aqueous solution.

Conflicts of interest

There are no conflicts to declare.

Acknowledgements

We gratefully acknowledge financial support from the Natural Science Foundation of China (21776181), Sichuan University innovation spark project (2018SCUH0012), Special Project of Building World-class Universities (2030704401004) and Special Fund Project for Cooperation between Sichuan University and Panzhihua City (2018CDPZH-21).

© 2021 The Author(s). Published by the Royal Society of Chemistry

References

1 M. A. Hashem, M. Hasan, M. A. Momen, S. Payel and M. S. Nur-A-Tomal, *Environ. Sustain. Indicat.*, 2020, **5**, 100022.
2 A. L. Arim, M. J. Quina and L. M. Gando-Ferreira, *Chem. Eng. Technol.*, 2018, **41**, 1378–1389.
3 A. Dabrowski, Z. Hubicki, P. Podkoscielny and E. Robens, *Chemosphere*, 2004, **56**, 91–106.
4 Z. Bahadır, V. N. Bulut, D. Ozdes, C. Duran, H. Bektas and M. Soylak, *J. Ind. Eng. Chem.*, 2014, **20**, 1030–1034.
5 P. Miretzky and A. F. Cirelli, *J. Hazard. Mater.*, 2010, **180**, 1–19.
6 W. Liu, H. Chen, A. G. L. Borthwick, Y. Han and J. Ni, *Chem. Eng. J.*, 2013, **232**, 228–236.
7 T. A. Kurniawan, G. Y. S. Chan, W.-H. Lo and S. Babel, *Chem. Eng. J.*, 2006, **118**, 83–98.
8 J. Kanagaraj, T. Senthilvelan, R. C. Panda, R. Aravindhan and A. B. Mandal, *Chem. Eng. Technol.*, 2014, **37**, 1741–1750.
9 M. S. El-Shahawi, S. S. M. Hassan, A. M. Othman and M. A. El-Sonbati, *Microchem. J.*, 2008, **89**, 13–19.
10 A. Zarezadeh, H. R. Rajabi, O. Sheydaei and H. Khajehsharifi, *Mater. Sci. Eng., C*, 2019, **94**, 879–885.
11 S. Alipour, P. A. Azar, S. W. Husain and H. R. Rajabi, *Sens. Actuators, B*, 2020, **323**, 128668.
12 M. B. Gholivand, M. Shamsipur, S. Dehdashtian and H. R. Rajabi, *Mater. Sci. Eng., C*, 2014, **36**, 102–107.
13 M. Shamsipur, H. R. Rajabi, S. M. Pourmortazavi and M. Roushani, *Spectrochim. Acta, Part A*, 2014, **117**, 24–33.
14 H. R. Rajabi, M. Shamsipur, M. M. Zahedi and M. Roushani, *Chem. Eng. J.*, 2015, **259**, 330–337.
15 K. Mukherjee, R. Saha, A. Ghosh and B. Saha, *Res. Chem. Intermed.*, 2012, **39**, 2267–2286.
16 W. He, K. Ai, X. Ren, S. Wang and L. Lu, *J. Mater. Chem. A*, 2017, **5**, 19593–19606.
17 N. Hidayati, D. R. Apriliani, Helda, T. Taher, R. Mohadi, Elfita and A. Lesbani, *J. Phys.: Conf. Ser.*, 2019, **1282**, 012075.
18 D. T. Hobbs, M. J. Barnes, R. L. Pulmano, K. M. Marshall, T. B. Edwards, M. G. Bronikowski and S. D. Fink, *Sep. Sci. Technol.*, 2005, **40**, 3093–3111.
19 M. J. Manos and M. G. Kanatzidis, *J. Am. Chem. Soc.*, 2012, **134**, 16441–16446.
20 D. Sarma, C. D. Malliakas, K. S. Subrahmanyam, S. M. Islam and M. G. Kanatzidis, *Chem. Sci.*, 2016, **7**, 1121–1132.
21 Z. Yang, F. Wang, C. Zhang, G. Zeng, X. Tan, Z. Yu, Y. Zhong, H. Wang and F. Cui, *RSC Adv.*, 2016, **6**, 79415–79436.
22 C. Li, M. Wei, D. G. Evans and X. Duan, *Small*, 2014, **10**, 4469–4486.
23 K. H. Goh, T. T. Lim and Z. Dong, *Water Res.*, 2008, **42**, 1343–1368.
24 Z. Gu, J. J. Atherton and Z. P. Xu, *Chem. Commun.*, 2015, **51**, 3024–3036.
25 R. Tian, R. Liang, M. Wei, D. G. Evans and X. Duan, *Struct. Bonding*, 2016, **172**, 65–84.
26 B. Zümreoglu-Karan and A. Ay, *Chem. Pap.*, 2012, **66**, 1–10.
27 D. Yang, H. Liu, Z. Zheng, S. Sarina and H. Zhu, *Nanoscale*, 2013, **5**, 2232–2242.
28 A. Dyer, M. Pillinger, R. Harjula and S. Amin, *J. Mater. Chem.*, 2000, **10**, 1867–1874.
29 W. Huang, S. Komarneni, A. R. Aref, Y. D. Noh, J. Ma, K. Chen, D. Xue and B. Jiang, *Chem. Commun.*, 2015, **51**, 15661–15664.
30 A. I. Bortun, S. A. Khainakov, L. N. Bortun, E. Jaimez, J. R. García and A. Clearfield, *Mater. Res. Bull.*, 1999, **34**, 921–932.
31 K. Wang, J. Gu and N. Yin, *Ind. Eng. Chem. Res.*, 2017, **56**, 1880–1887.
32 L. Khezami and R. Capart, *J. Hazard. Mater.*, 2005, **123**, 223–231.
33 J. H. Chen, H. T. Xing, H. X. Guo, G. P. Li, W. Weng and S. R. Hu, *J. Hazard. Mater.*, 2013, **248–249**, 285–294.
34 S. Guilane and O. Hamdaoui, *Desalin. Water Treat.*, 2015, **57**, 15826–15834.
35 J. Liu, X. Wu, Y. Hu, C. Dai, Q. Peng and D. Liang, *J. Chem.*, 2016, **2016**, 1–11.
36 Z.-h. Yang, B. Wang, L.-y. Chai, Y.-y. Wang, H.-y. Wang and S. Chang-qing, *J. Cent. South Univ.*, 2008, **16**, 0101–0107.
37 W. S. W. Ngah, A. Kamari, S. Fatinathan and P. W. Ng, *Adsorption*, 2006, **12**, 249–257.
38 X. S. Wang, Z. Z. Li and S. R. Tao, *J. Environ. Manage.*, 2009, **90**, 721–729.
39 T. Wang, W. Liu, L. Xiong, N. Xu and J. Ni, *Chem. Eng. J.*, 2013, **215–216**, 366–374.
40 I. Langmuir, *J. Am. Chem. Soc.*, 1918, **40**, 1361–1403.
41 H. M. F. Freundlich, *Z. Phys. Chem. A*, 1906, **57**, 385–470.
42 R. Vala, D. Wankasi and E. Dikio, *Hem. Ind.*, 2016, **70**, 565–572.
43 Y. S. Ho and G. McKay, *Process Biochem.*, 1999, **34**, 451–465.
44 X. He, X. Min and X. Luo, *J. Chem. Eng. Data*, 2017, **62**, 1519–1529.
45 A. Dzieniszewska, J. Kyziol-Komosinska and M. Pająk, *PeerJ*, 2020, **8**, 22.
46 T. Ai, X. Jiang and Q. Liu, *Open Chem.*, 2018, **16**, 842–852.
47 J. D. Castro-Castro, N. R. Sanabria-González and G. I. Giraldo-Gómez, *Data Brief*, 2020, **28**, 105022.
48 J. Qiu, X. Du, S. Komarneni, H. Wang, X. Cheng and Z. Du, *J. Appl. Polym. Sci.*, 2020, **137**, e49065.
49 G. Wójcik, *Materials*, 2020, **13**, 2256.
50 X. Wang, S. Cui, B. Yan, L. Wang, Y. Chen and J. Zhang, *J. Wuhan Univ. Technol., Mater. Sci. Ed.*, 2019, **34**, 587–595.
51 W. Peng, S. Du, Z. Shaoning, H. Xieyi, B. Qingyuan, Q. Meng, Z. Wei and H. Fuqiang, *J. Hazard. Mater.*, 2020, **384**, 121278.
52 W. Cui, X. Zhang, C. I. Pearce, Y. Chen, S. Zhang, W. Liu, M. H. Engelhard, L. Kovarik, M. Zong, H. Zhang, E. D. Walter, Z. Zhu, S. M. Heald, M. P. Prange, J. J. De Yoreo, S. Zheng, Y. Zhang, S. B. Clark, P. Li, Z. Wang and K. M. Rosso, *Environ. Sci. Technol.*, 2019, **53**, 11043–11055.

© 2021 The Author(s). Published by the Royal Society of Chemistry